Effect of Baseline Separation Distance on GMT Velocity Estimation using Monopulse GMTI Technique in case of SAR

[1]Vandana AR,[2]Dr CR Byra Reddy
[1]Research Scholar,[2]Professor
[1]Department of ECE,
[1]Bangalore Institute of Technology, Bangalore, Karnataka,India

***Abstract*—This paper discusses the effect of Baseline separation distance on GMT (Ground Moving Target) velocity estimation using Monopulse GMTI (Ground Moving Target Indication)technique in case of airborne SAR. The simulation results of the same has been presented.Unambiguity inestimated target velocity due to increase in baseline separation distance between the antenna phase center > λ/2 in case of monopulse SAR is discussed. The baseline separation distance impacts the target velocity due to under sampling of target phase information. It also impact the squint doppler which adds to the estimated target Doppler thereby effecting the ground moving target velocity estimation. Doppler spread in range due to the relative motion of target and platform velocity is not considered here as it does not have much impact on velocity estimation using Monopulse GMTI method.**

***IndexTerms*—SAR, GMTI, Monopulse, Baseline separation distance, Monopulse Doppler squint, SNR**

I. INTRODUCTION

Synthetic Aperture Radar synthesis large antenna using smaller antenna by collecting the received echoes from different positions as shown in Figure 1. The collected received echoes are then synthesized to form a single antenna to get high resolution which is useful in case of GMT detection and imaging. The geometry of SAR is shown in Fig 1 where Vs is the platform velocity, d is the distance moved by the antenna between two transmitted pulses, Ro is the slant range, h is the height of the platform, x-axis is the slow time, y-axis is fast time.Consider the string of dots in Figure 1 which shows the position at which the SAR transmits a pulse. Each pulse saves the phase histories of the response at each position as the beam moves through the scene. On the received pulses motion compensation, range compression and azimuth compression algorithms are applied to obtain focused SAR data. However motion compensation, range compression and azimuth compression are out of scope of this work. The method discussed is based on focused SAR range Doppler data. Latest literatures use MPR (MonoPulseRatio) to detect the GMT which gives optimum clutter cancellation and better GMT velocity estimation [1] called Monopulse GMTI technique. Analysis in this paper are with respect to Monopulse GMTI technique.

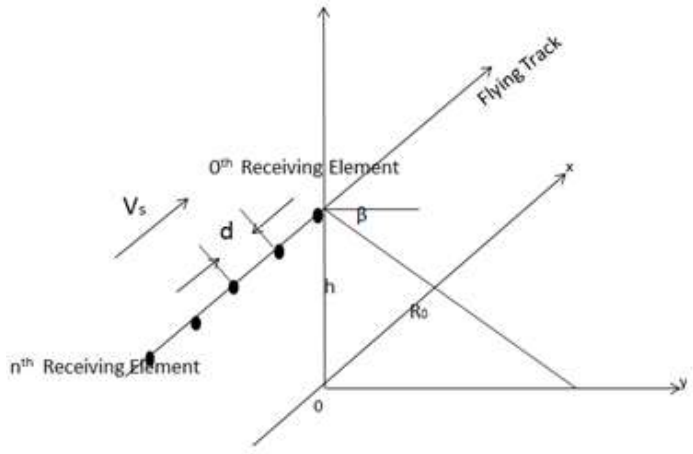

Figure 1: Geometry of Synthetic Aperture Radar

II. THEORETICAL ASPECT

Let us consider the moving platform as in case of airborne radar shown in Figure 1. When the platform is moving the look angle from the radar with respect to the target changes. Due to this change in look angle, target doppler as seen by the radar also changes. Let us consider the case of monopulse SAR where each look angle receives two returns from two phase centers along azimuth direction or cross range direction. Geometry of Monopulse SAR for one look angle is shown in Fig 2 where d is

the baseline separation distance between two phase centers, θ is the angle subtended by the target from the phase centers, Ro is the slant range. Fig 2 shows that the two phase centers of phase comparison monopulse system experiences different phase shifts which is dependent on d and θ angle of the radar with respect to the target.

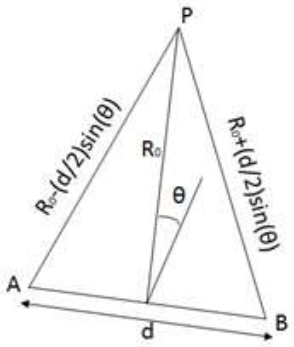

Figure 2: Geometry of Monopulse Antenna in Azimuth direction

The Monopulse SAR geometry across the pulses is shown in Fig 3 where $S_1$and S_2 are the positions of antenna phase centerA and Brespectively with respect to P, position of the target.

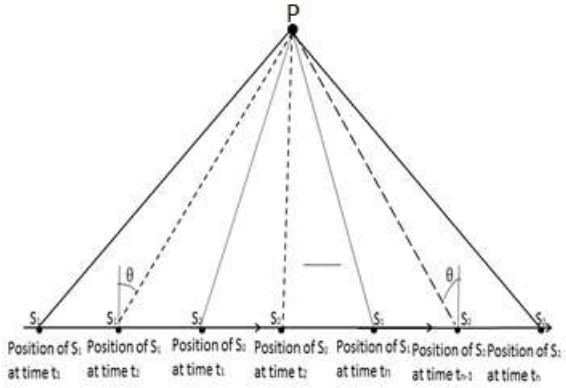

Figure 3: Geometry of Monopulse SAR

Using Fig 3 and Fig 2 signals S_{c1} and S_{c2}received by antenna phase centers A and B respectively can be given as in Eqn (1) and Eqn(2).

$$S_{c1}(n) = e^{j(4\pi V_r tn/T/\lambda)}\ e^{j\phi 0} e^{\frac{+j2\pi d\sin(\theta)}{\lambda}} \quad (1)$$

$$S_{c2}(n) = e^{j(4\pi V_r tn/T/\lambda)}\ e^{j\phi 0} e^{\frac{-j2\pi d\sin(\theta)}{\lambda}} \quad (2)$$

Where

V_r= Target Radial Velocity
θ=Aspect Angle (±45deg) which changes across the pulses
λ= Wavelength
d = Baseline separation distance between the antenna
t=PRT time
n = Sample number
T=Dwell time
$\phi 0=\frac{4\pi R0}{\lambda}$ is the phase due to slant range

$\phi 0$is constant and can be eliminated for analysis purpose as it contributes only to the amplitude part.

Eqn (1) and Eqn(2) can be rewritten in frequency domain as

$$S_{c1}(\omega) = e^{\omega+\omega 0} \quad (3)$$

$$S_{c2}(\omega) = e^{\omega-\omega 0} \quad (4)$$

Where

$$\omega = \text{Target Doppler} = 2\pi f_r \quad (5)$$

with f_r = target doppler

$$\omega 0 = \text{Squint Doppler} = 4\pi\sin(\theta)Vs/\lambda \quad (6)$$

Squint Doppler is caused due to the baseline separation distance which varies with respect to the angle of the radar from the target. The monopulseSum(Σ) and Delta(Δ) channels can be written as in Eqn (7) and Eqn(8).

$$\Sigma(\omega)=e^{\omega+\omega 0}+e^{\omega-\omega 0} \quad (7)$$

$$\Delta(\omega)= e^{\omega+\omega 0}-e^{\omega-\omega 0} \quad (8)$$

Let

$$a= \omega + \omega 0 \quad (9)$$

$$b= \omega - \omega 0 \quad (10)$$

$$\frac{(e^a\ (1\ -e^{b/a}))}{(e^a\ (1\ +e^{b/a}))} \quad (11)$$

Let

$$y=b/a \quad (12)$$

$$=\frac{1\ -e^y}{1\ +e^y} =\frac{1\ -e^{y/2}e^{y/2}}{1\ +e^{y/2}e^{y/2}}= \frac{e^{\frac{y}{2}}(e^{-\frac{y}{2}}-e^{\frac{y}{2}})}{e^{\frac{y}{2}}(e^{-\frac{y}{2}}+e^{\frac{y}{2}})} \quad (13)$$

$$\frac{\Delta(\omega)}{\Sigma(\omega)} = \tanh\left(\frac{b}{2a}\right) \quad (14)$$

$$\text{MPR}= \frac{\Delta(\omega)}{\Sigma(\omega)} = \tanh\left(\frac{\omega-\omega 0}{2(\omega+\omega 0)}\right) \quad (15)$$

The plot of Eqn (15)i.e MPRfor target velocity -100m/s, lambda=0.031m, with platform velocity 100m/s is shown in Fig 4 below.The plot of Eqn (15) for target velocity varying from 10 to 50m/s, lambda=0.031m, with platform velocity =-100m/s is shown in Fig 5 below.

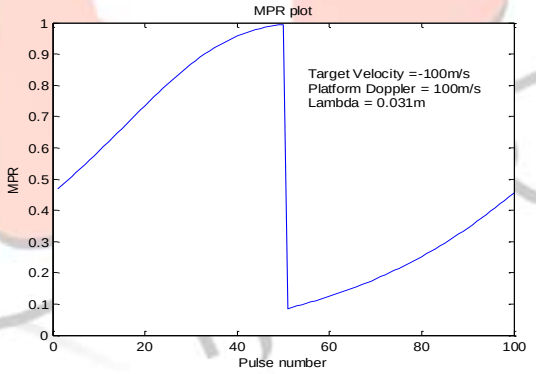

Figure 4:MPR plot using Eqn(15)

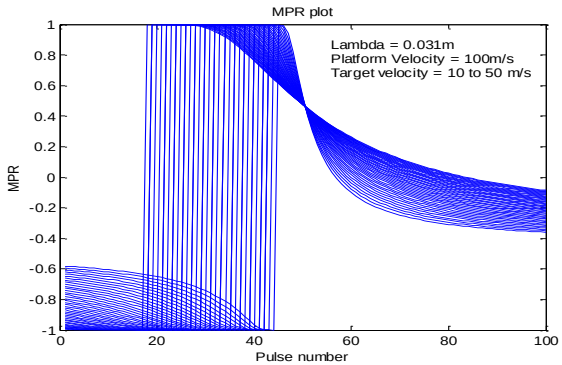

Figure 5:MPR plot using Eqn (15) for target velocities varying from 10 to 50 m/s

From Fig 4 and Fig 5 it can be concluded that the tanh (MPR) function startat target doppler (ω). Therefore the target Doppler can be estimated by looking at the position of tanh (MPR) function

Now let us consider the condition for baseline separation distance impact on MPR. We know that baseline separation distanceshould satisfy Eqn (16) to get unambiguous target velocity estimation.

$$d \leq \frac{\lambda V_s}{2V_r} \qquad (16)$$

To know what happens for baseline separation distance d> than the value given in Eqn(16) let us look at Eqn(5), (6) and (16). By analyzing these Eqn'swe can conclude thatMPRin Eqn(15) start to fold and also MPR becomes ambiguous for baseline separation distance d greater than the value given in Eqn(16). Therefore velocity estimation using MonopulseGMTI technique also becomesambiguous for baseline separation distance d greater than the value in Eqn(16). To better understand the ambiguity in monopulse ratio simulations for different baseline separation distances and different wavelength and different target velocities were performed. The simulation results and the theoretical aspects are found to be matching. The simulation results are shown in next section.

III. Simulation Results

Simulation results of ambiguous MPRand thereby doppler estimate due to the variation in target doppler and squint doppler because of increase in d in case of monopulseSAR is shown in this section. The parameters used for simulation are listed below

- X, Ka, and Ku band,
- Separation distance λ/2, λ, 2λ, 4λ,
- Slant Range is 60Km,
- Max Angle Coverage is +/-45°,
- Target Velocity varying from -100m/s to +100 m/s.
- $\frac{V_s}{V_r}$ =1

Eqn(1) and Eqn(2) are used to generate focused SAR signal returns from two channels A and B as shown in Fig 2. FFT is performed on the signals and the MPR is calculated in frequency domain. Using MPR target doppler will be estimated. MPR follows tanh function with peak at target doppler. Simulation results are shown from Figure 6 to Figure 25.[4], [5], [6], [7], [8] are some of the literature referred for simulation and analysis.

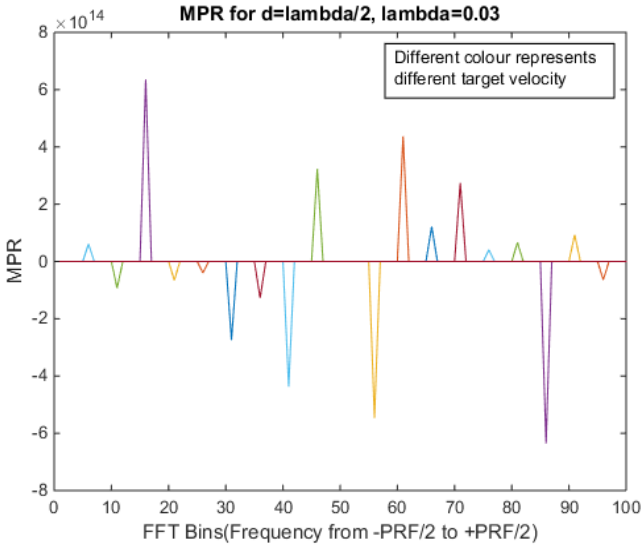

Figure 6: Plot of MPR for d=λ/2 with λ=0.03

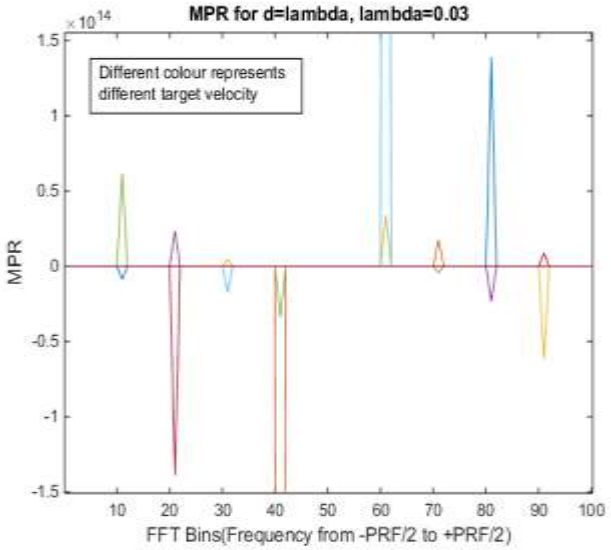

Figure 7: Plot of MPR for d=λ with λ=0.03

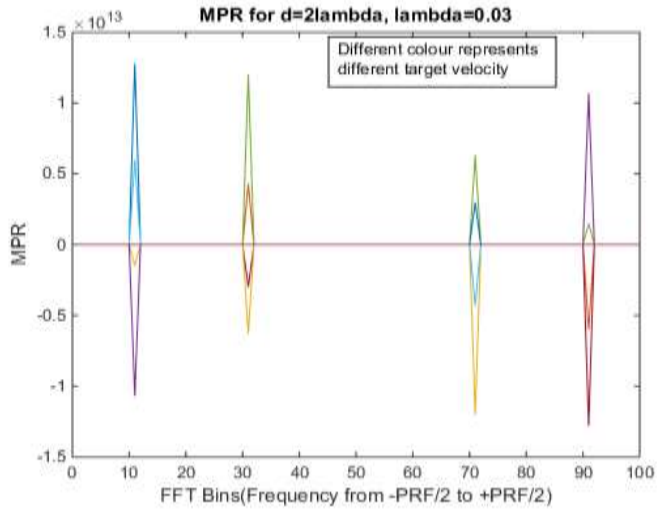

Figure 8: Plot of MPR for d=2λ with λ=0.03

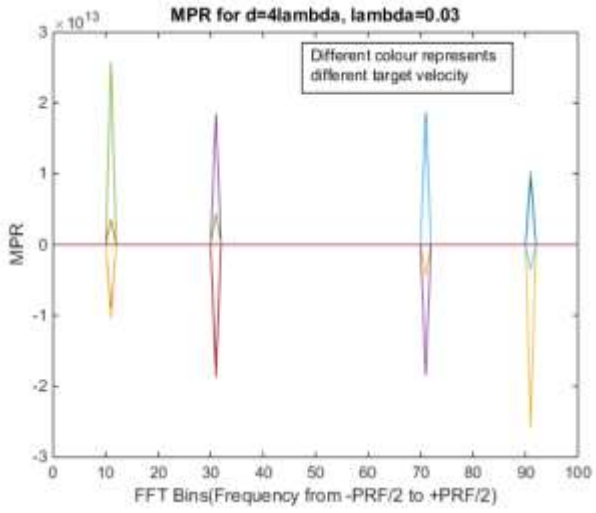

Figure 9: Plot of MPR for d=4λ with λ=0.03

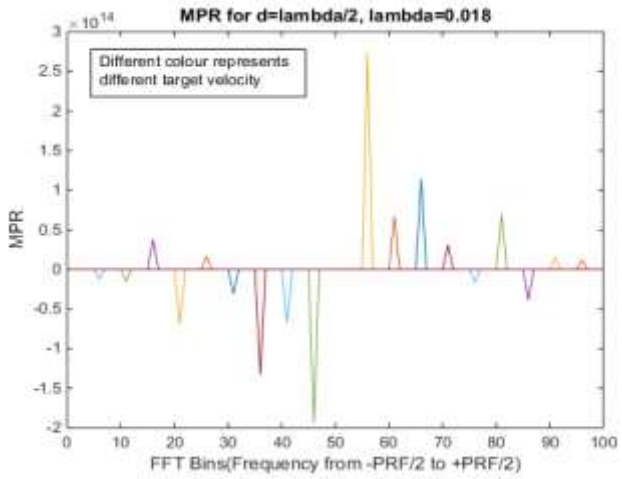

Figure 10: Plot of MPR for d=λ/2 with λ=0.018

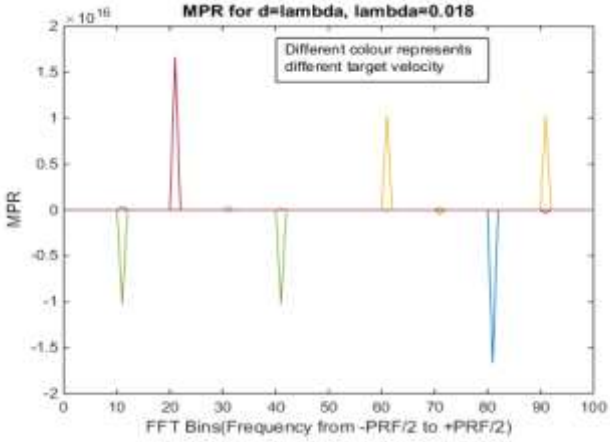

Figure 11: Plot of MPR for d=λ with λ=0.018

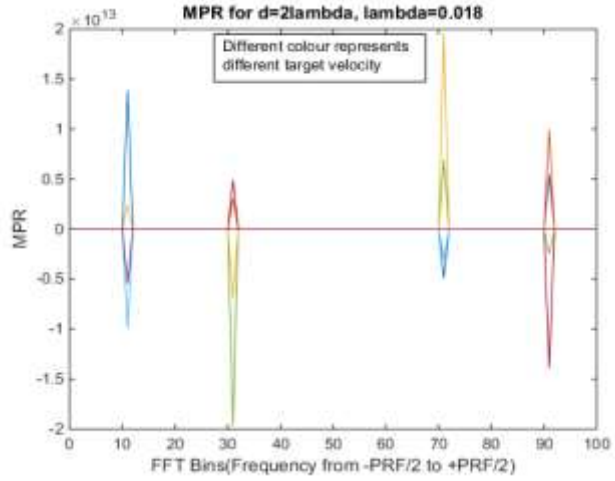

Figure 12: Plot of MPR for d=2λ with λ=0.018

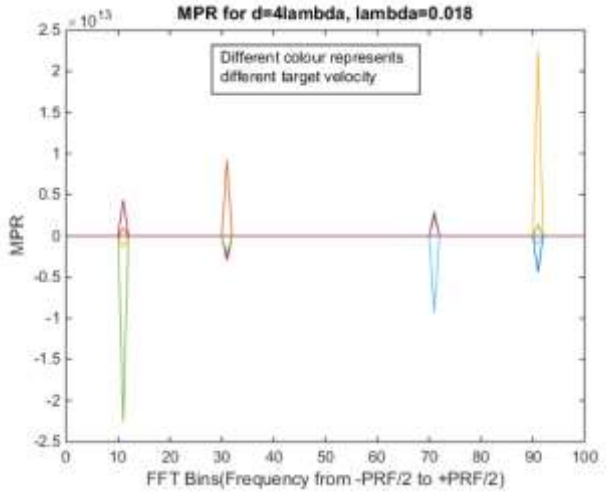

Figure 13: Plot of MPR for d=4λ with λ=0.018

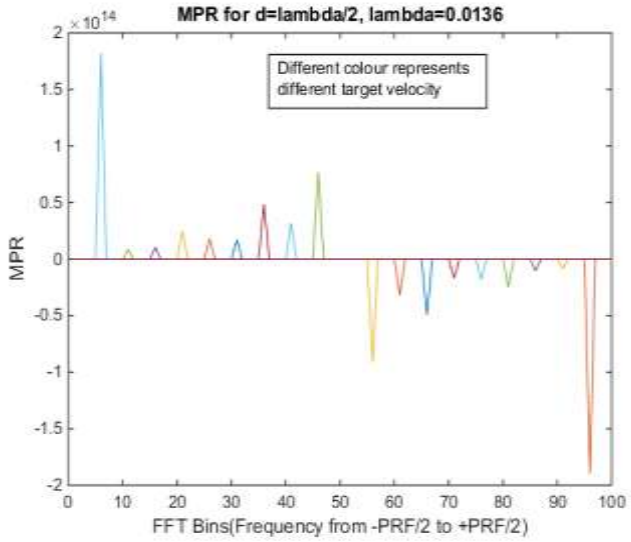

Figure 14: Plot of MPR for d=λ/2 with λ=0.0136

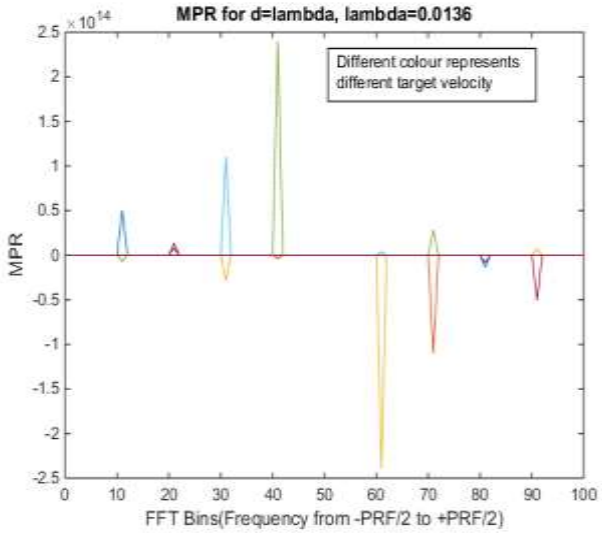

Figure 15: Plot of MPR for d=λ with λ=0.0136

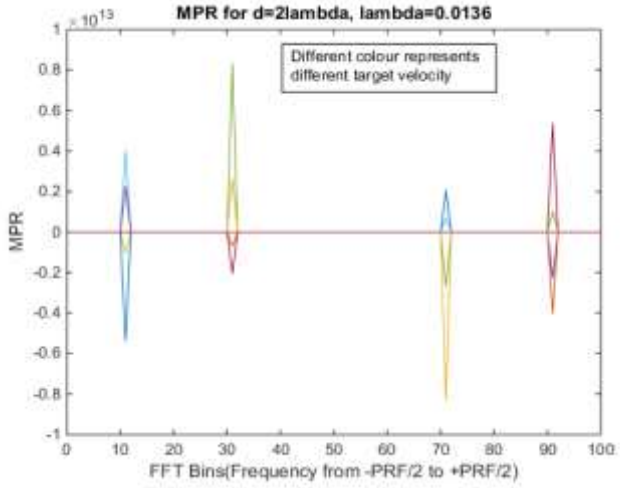

Figure 16: Plot of MPR for d=2λ with λ=0.0136

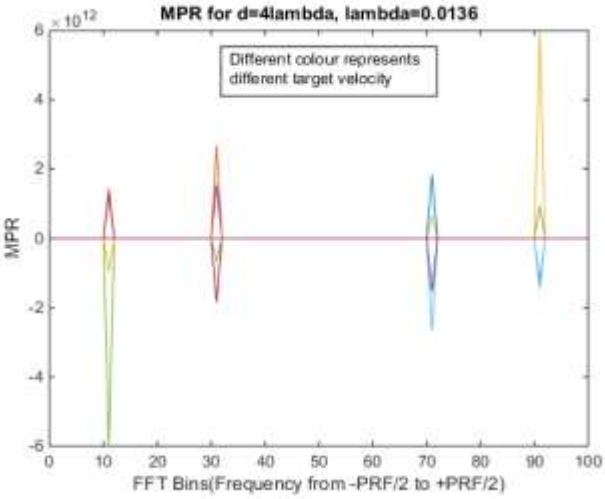

Figure 17: Plot of MPR for d=4λ with λ=0.0136

Figure 14 shows the plot of MonoPulse Ratio (MPR) for d=λ/2 with λ=0.0136. Figure 15 shows the plot of MonoPulse Ratio (MPR) for d=λ with λ=0.0136. Figure 16 shows the plot of MonoPulse Ratio (MPR) for d=2λ with λ=0.0136. Figure 17 shows the plot of MonoPulse Ratio (MPR) for d=4λ with λ=0.0136.

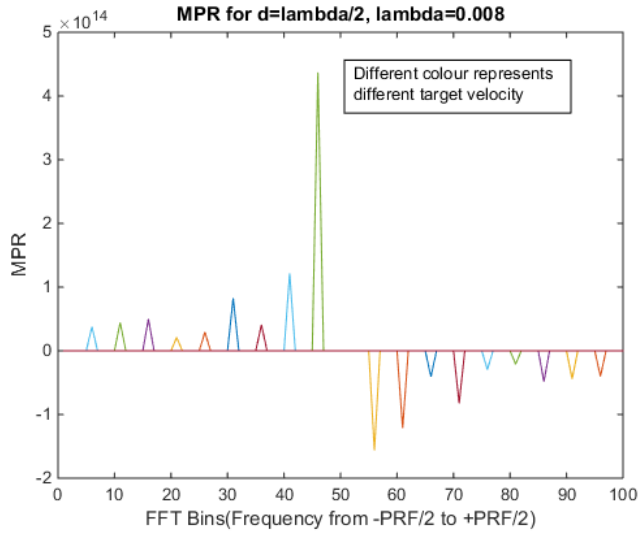

Figure 18: Plot of MPR for d=λ/2 with λ=0.008

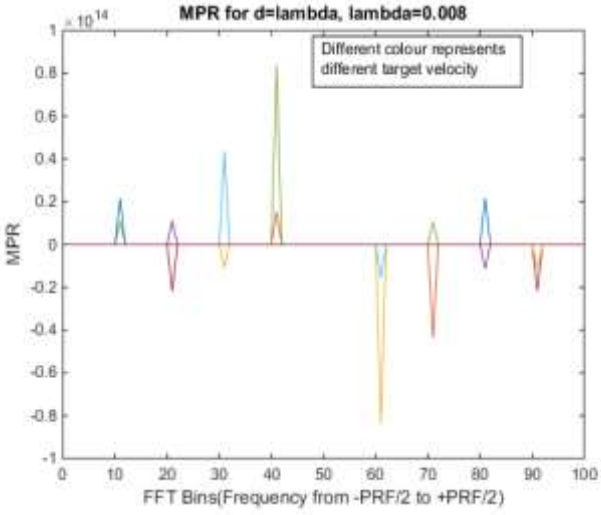

Figure 19: Plot of MPR for d=λ with λ=0.008

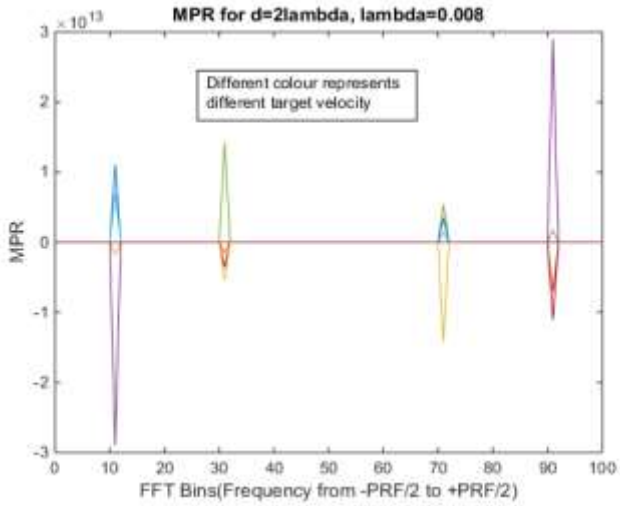

Figure 20: Plot of MPR for d=2λ with λ=0.008

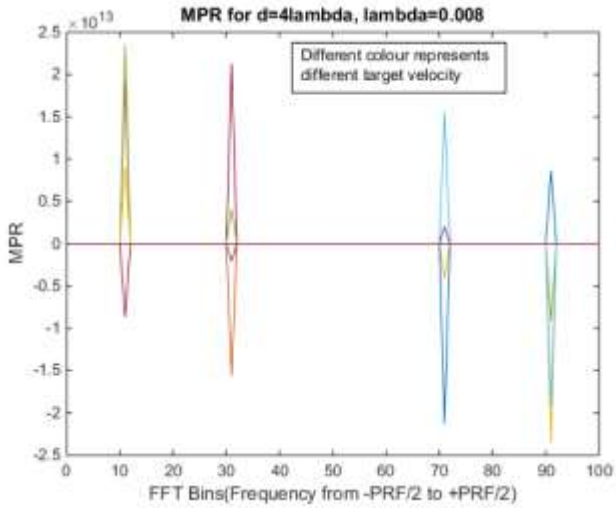

Figure 21: Plot of MPR for d=4λ with λ=0.008

Figure 18 shows the plot of MonoPulse Ratio (MPR) for d=λ/2 with λ=0.008. Figure 19 shows the plot of MonoPulse Ratio (MPR) for d=λ with λ=0.008. Figure 20 shows the plot of MonoPulse Ratio (MPR) for d=2λ with λ=0.008. Figure 21 shows the plot of MonoPulse Ratio (MPR) for d=4λ with λ=0.008.

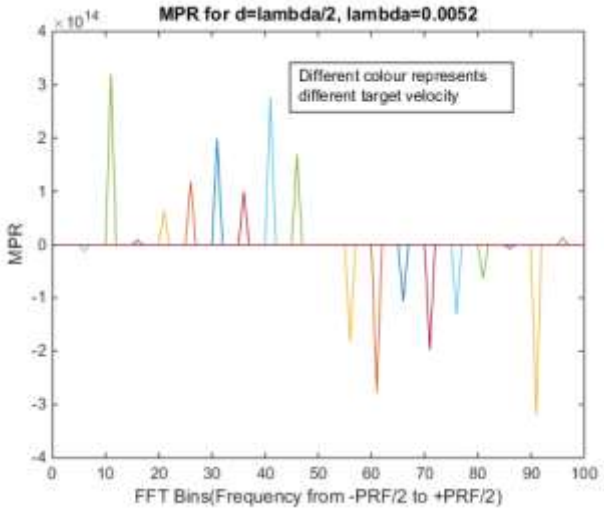

Figure 22: Plot of MPR for d=λ/2 with λ=0.0052

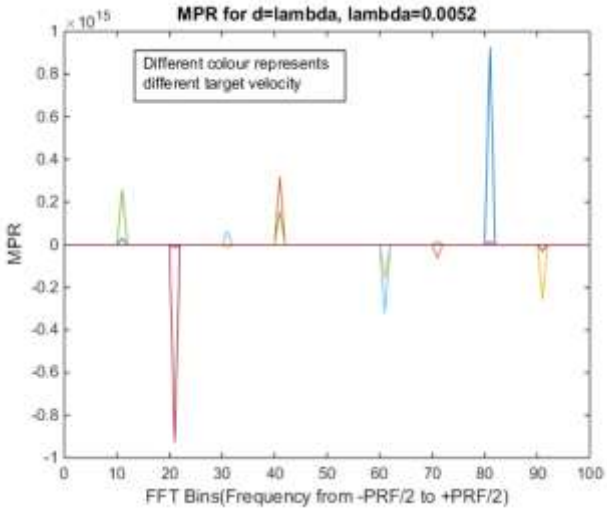

Figure 23: Plot of MPR for d=λ with λ=0.0052

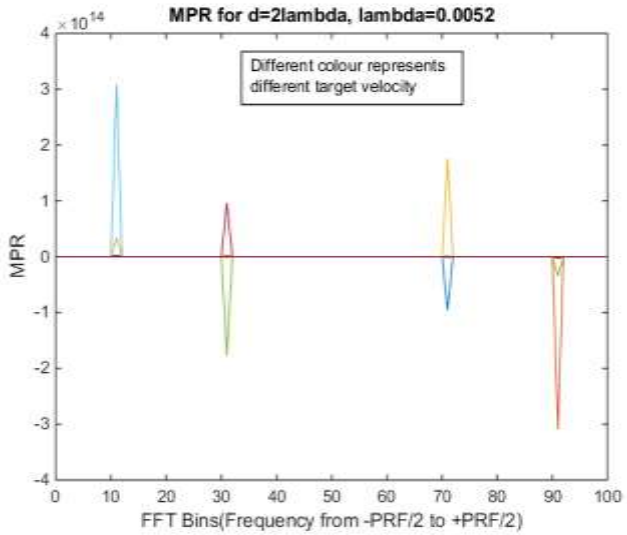

Figure 24: Plot of MPR for d=2λ with λ=0.0052

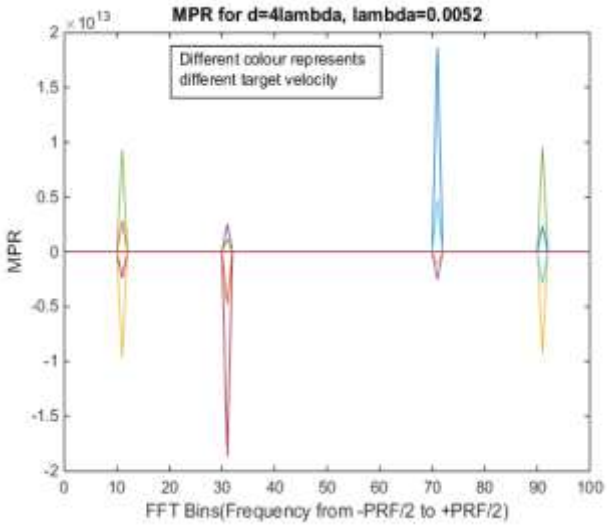

Figure 25: Plot of MPR for d=4λ with λ=0.0052

Figure 22 shows the plot of MonoPulse Ratio (MPR) for d=λ/2 with λ=0.0052. Figure 23 shows the plot of MonoPulse Ratio (MPR) for d=λ with λ=0.0052. Figure 24 shows the plot of MonoPulse Ratio (MPR) for d=2λ with λ=0.00852. Figure 25 shows the plot of MonoPulse Ratio (MPR) for d=4λ with λ=0.0052. It can be concluded that the MPR folds for d>λ/2 as expected from the theory. Hence velocity estimation using Monopulse GMTI technique becomes ambiguousfor d>λ/2.

IV. CONCLUSION

This paper discusses the variation of target doppler and the squint doppler with respect to baseline separation distance between the phase centers in case of Monopulse SAR. This analysis is useful in estimating target velocity using Doppler monopulse ratio in case of SAR. Simulation results ofmonopulseratio for different operating frequency and different phase center separation distance are shown. Relation between target doppler and the squint doppler with respect to baseline separation distance between the monopulsephase centers is discussed.

V. FUTURE SCOPE

Other methods to estimate target Doppler and squint Doppler on MPR can be explored.

REFERENCES

[1] Maurice Ruegg, Erich Meier, Daniel Nuesch, "Capabilities of Dual-Frequency Millimeter wave SAR with monopulse for Ground Moving Target Indication", IEEE Transactions on Geoscience and Remote Sensing (Volume: 45, Issue: 3, March 2007).

[2] Jia Xu, Yu Zuo, Bin Xia, Xiang-Gen Xia, Yung-Ning Peng, and Yong-Liang Wang, "Ground Moving Target Signal Analysis in Complex Image Domain for Multichannel SAR", IEEE Transactions On Geoscience and Remote Sensing, Vol. 50, No 2, February 2012.

[3] Mark A Richards "Fundamentals of Radar Signal Processing" McGraw-Hill

[4] Sune R. J. Axelsson "Position Correction of moving target in SAR-imagery", Proceedings of SPIE, Vol. 5236, 2004

[5] Shen Chiu, "Clutter effects on ground moving Target Velocity Estimation with SAR Along-track Interferometry", IGARSS, 2003

[6] S M Sherman and D K Barton, "Monopulse Principles and Techniques", Artech House Publishers 2011.

[7] Richard G Lyons, "Understanding Digital Signal Processing" 2001.

[8] M I Skolnik, "Radar Handbook", NewYork Hill, 3rd Edition, 2008.